

This is a postprint version of the following published document:

Albarracín-Vargas, Fernando; González-Posadas, Vicente; Herráiz-Martínez, Francisco Javier; Segovia-Vargas, Daniel (2016). Design Method for Actively Matched Antennas with Non-Foster Elements. *IEEE Transactions on Antennas and Propagation*, 64(9), pp.: 4118-4123.

DOI: <https://doi.org/10.1109/TAP.2016.2583482>

© 2016 IEEE. Personal use of this material is permitted. Permission from IEEE must be obtained for all other uses, in any current or future media, including reprinting/republishing this material for advertising or promotional purposes, creating new collective works, for resale or redistribution to servers or lists, or reuse of any copyrighted component of this work in other works.

See <https://www.ieee.org/publications/rights/index.html> for more information.

## Design Method for Actively Matched Antennas with Non-Foster Elements

Fernando Albarracin-Vargas, Vicente Gonzalez-Posadas, F.J. Herraiz-Martinez, and Daniel Segovia-Vargas, *Member IEEE*

**Abstract**— The design of electrically small antennas loaded with active non-Foster elements is a topic whose interest has grown in the last years. In this paper, a new strategy for the design of actively matched antennas loaded with non-Foster elements is presented. The analysis of different parameters, such as the sensitivity to non-Foster circuit placement, the overall antenna system stability and current distributions, has to be considered in order to enhance the antenna performance. A design example using an electrically small antenna (ESA) and its realization is presented to validate the proposed strategy.

**Index Terms**— Non-Foster Reactance, Stability, Small-Antennas, Active Matching Networks.

### I. INTRODUCTION

ACTIVE and non-Foster matching networks (MN) can be an attractive alternative for electrically small antennas (ESA) design. The current demand on more compact and broader bandwidth antennas make necessary to improve the performance of ESAs. A smart strategy for including non-Foster networks in ESAs, helping to overcome their inherent stability problems while optimizing its placement in the antenna, will always be welcome in communications systems that integrate broadband with compact size antennas

A fundamental limit, first derived by Wheeler [1], Chu [2], and Thal [3] imposes a minimum feasible quality factor  $Q$  for a certain antenna physical size. Therefore, an ESA is assumed to have high- $Q$  impedance, characterized by large reactance and small radiation resistance. On the other hand, the design of a passive MN for an ESA is limited to the gain-bandwidth criteria, imposed by Bode [4], Fano [5] and Youla [6]. This criterion states that it is possible to achieve well a given gain in a very small bandwidth (by matching the antenna with lossless capacitors and inductors), well larger bandwidths by including losses in the MN, but resulting in a very poor efficiency and, hence, low gain. These limitations make this class of antennas, in general, be structures difficult to match.

The inclusion of active elements in the matching network, well in the antenna structure itself well in a near-field parasitic element, can allow overcoming the previous constraints. These components do not obey the Foster theorem [7] and can compensate the reactance of the antenna by implementing a decrease of its reactance with the frequency allowing to match the antenna along broader bandwidths [8]. These non-Foster

elements, namely negative capacitors, and inductors, are realized by using 2-port active circuits so-called Negative Impedance Convertors (NICs) [9] or Negative Impedance Inverters (NIIs) [10]. A NIC is a 2-port active circuit, in which one port presents a negated (and possibly inverted) version of the impedance loading the other port.

Previously reported works mostly include using of non-Foster components at the terminals of dipole or monopole like antennas [8], [11]. An ideal approach would imply two or three non-Foster elements in series with the antenna and some reactive circuit to transform the frequency-squared-dependent resistance of the antenna into a constant resistance (e.g. 50  $\Omega$ ). It is clear that actual feasibility of this option is limited [8] mainly due to stability problems.

Another approach is to embed a non-Foster element into a resonant antenna [12]-[14]. Two different strategies have followed this line. The first one consists on including the non-Foster network inside the antenna itself to obtain a broadband matched antenna by shaping the current distributions on the antenna [12]. In the second one, the design procedure departs from a metamaterial-inspired antenna, and then the inclusion of a variable reactance that achieves a reactively tunable antenna (also known as *frequency-agile*) through the variation of an embedded passive tuning element (i.e. conventional capacitance or inductance) [13]-[14]. From the frequency-agile antenna, the needed reactance to achieve broadband performance can be extracted. This reactance can be obtained by the inclusion of a non-Foster circuit.

Instead of considering particular and different metamaterial inspired antennas to be integrated with non-Foster circuits, the present work aims at proposing a global methodology for the design of actively matched antennas. In this way, the antenna and the non-Foster networks are considered as a whole system. In addition to the impedance bandwidth improvement, the stability and tolerance of the components, the current distributions and the corresponding radiation patterns will also be considered.

This paper is organized as follows: Section II describes the proposed strategy. Section III shows a design example applying the proposed methodology to a printed small semi-loop, loaded with a MOSFET-based NII as active MN. Finally, a discussion of the results is presented in Section IV

### II. NON-FOSTER ACTIVE MATCHING ANTENNA DESIGN

In this section, the proposed strategy is described. First, the antenna to be integrated with a non-Foster circuit undergoes a sensitivity analysis to see whether the antenna is suitable for it or not; in addition, this sensitivity analysis will also determine the most appropriate place for the NIC. Secondly, not all the

F. Albarracin-Vargas, F.J. Herraiz-Martinez and D. Segovia-Vargas are with the Department of Signal Theory and Communications, Carlos III University of Madrid (UC3M), 29811 Leganés, Madrid, Spain (e-mail: [fabarracin@tsc.uc3m.es](mailto:fabarracin@tsc.uc3m.es), [dani@tsc.uc3m.es](mailto:dani@tsc.uc3m.es)). V. Gonzalez-Posadas is with

Department of Signal Theory and Communications, Polytechnic University of Madrid (UPM), 28031, Madrid, Spain (e-mail: [ygonzalz@diac.upm.es](mailto:ygonzalz@diac.upm.es)). This work has been partially granted by MINECO under the project TEC2013-47753-C3-2-R and RTC 2014-2380-4.

non-Foster networks are valid for being integrated with the antenna, so some remarks on the non-Foster network are provided in order to choose the most suitable one. Third, a trustworthy stability analysis of the overall structure (NIC + antenna) has to be done; it is important to emphasize that the analysis has to be done in the overall structure since the antenna loading can modify the overall performance of the NIC stability. Fourth, the radiation pattern of the integrated antenna has to be studied; this analysis is undertaken by studying the variations of the current distributions in the original antenna. Finally, since any change in the actual value of the components in the NIC can modify the performance, well in stability well in sensitivity of the overall structure, a tolerance analysis is welcome in order to predict potential and uncontrolled variations. Figure 1 shows a sketch of the previously described design strategy.

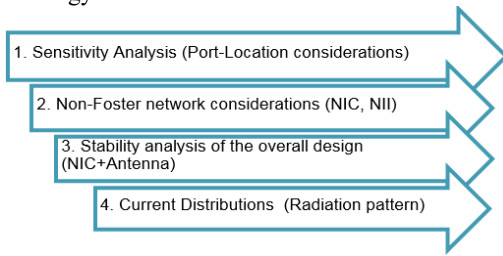


Fig. 1. Summary of the proposed strategy.

#### A. Step 1: Sensitivity analysis

The two-port antenna approach [15], sketched in Fig. 2, is used to deduce first, the suitability of the proposed antenna and then, the most convenient port location for the resulting 2-port network [16]. A second port is added to the antenna itself to be modeled in an electromagnetic CAD software, which has to be able to provide the  $S$ -parameters of different two-port combinations. This second port is the place inside the antenna where the non-Foster network is to be put. It should be pointed out that there is no need of an analytical circuit model for the antenna, difficult to extract in practice; this fact facilitates and generalizes the design process to other types of antennas

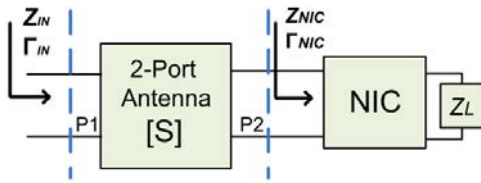


Fig. 2. Active matching with the two-port antenna approach.  $Z_L$  is the reactive load to be inverted by the NIC.

Once the new 2-port structure is available, the reflection coefficient at the input,  $\Gamma_{IN}$ , is given by (1).

$$\Gamma_{IN} = S_{11} + \frac{S_{12} \cdot S_{21} \cdot \Gamma_{NIC}}{1 - S_{22} \cdot \Gamma_{NIC}} = 0 \quad (1)$$

Since the goal is to have a matched antenna over a desired bandwidth the input reflection coefficient should be zero along this bandwidth. After some calculations and equating (1) to zero, we can obtain the optimum and analytical reflection

coefficient that the NIC (or NII) should provide,  $\Gamma_{IN}^{an}$ , as follows:

$$\Gamma_{NIC}^{an} = \frac{S_{11}}{S_{22} \cdot S_{11} - S_{12} \cdot S_{21}} \quad (2)$$

This impedance can be expressed in terms of the  $S$ -parameters of the 2-port antenna too, as follows:

$$Z_{NIC}^{an} = Z_0 \cdot \left( \frac{S_{22} \cdot S_{11} - S_{12} \cdot S_{21} + S_{11}}{S_{22} \cdot S_{11} - S_{12} \cdot S_{21} - S_{11}} \right) \quad (3)$$

If this impedance  $Z_{NIC}^{an}$  is placed at port 2, the reflection coefficient at port 1,  $\Gamma_{IN}$ , would ideally equal 0 at all frequencies and, hence, broad bandwidths could be obtained. However, due to the fact that the NIC input impedance is quite sensitive to variations in its load impedance ( $Z_L$  in Fig. 2) [9], it is also very important to analyze how these changes affect the overall input impedance. A new parameter such as the sensitivity,  $Sens$  (shown in 4), can help on this goal

$$\Delta \Gamma_{IN} = \frac{\partial \Gamma_{IN}}{\partial \Gamma_{NIC}} \Big|_{\Gamma_{NIC} = \Gamma_{NIC}^{an}} \Delta \Gamma_{NIC} = \frac{\Delta \Gamma_{NIC}}{Sens} = Sens \cdot \Delta \Gamma_{NIC} \quad (4)$$

The sensitivity,  $Sens$ , can be easily obtained by applying (4) to (1). From (5), it can be seen how  $Sens$  only depends on the  $S$ -parameters of the two-port antenna.

$$Sens = \left| \frac{S_{21} S_{12}}{(1 - S_{12} \Gamma_{NIC}^{an})^2} \right|_{\Gamma_{NIC} = \Gamma_{NIC}^{an}} = \left| \frac{(S_{11} S_{22} - S_{21} S_{12})^2}{S_{21} S_{12}} \right| \quad (5)$$

This parameter has to be calculated for different potential positions for the second port of the antenna where the NIC is to be loaded. The optimum choice is that where the sensitivity is minimized (it implies that changes in the NIC will not affect the input impedance). Otherwise, any small change in the impedance provided by the NIC will dramatically affect the antenna performance in terms of the impedance bandwidth.

#### B. Step 2: NIC Topology Considerations

The NIC selection comprises not only the frequency range of operation of transistors, where the upper bound of interest is used to be a tenth of the common high-frequency parameter,  $f_T$  (the gain bandwidth product defined as that frequency at which  $h_{fe} = 1$  (0 dB)) but the type of circuit connection. In this sense, floating or grounded NIC (or NII) configurations may be selected depending on the sensitivity analysis results. Then, if the lowest sensitivity point in the antenna is found to be near the ground plane (if it exists), a grounded configuration will be easier to build, especially for the DC return path from the bias network. Nevertheless, grounded configuration produces important changes in the current distribution of the antenna, especially in planar structures [16]. This implies that for antennas such as patches or printed monopoles, undesired changes in the radiation pattern of the actively matched antenna can arise. Among these changes, it could be mentioned

additional lobes or nulls and an entire different radiation mode. This phenomenon is due to the presence of an additional path to ground for the currents at frequencies where the NIC is currently working.

On the other hand, floating NIC configuration produces substantially lower changes in the radiation pattern, but with the drawback of higher values of sensitivity that implies, as aforementioned, poor impedance matching performance. In addition, larger stability problems may also arise for floating structures [8], [9]. Then a trade-off for the NIC selection has to be made to choose, both, the transistor (by considering its transition frequency) and the topology (grounded or floating) for the NIC, taking in mind the location of the lowest sensitivity point in the antenna structure.

### C. Step 3: Stability Analysis

The stability analysis is critical when non-Foster circuits are present. The situation when including the non-Foster circuit inside the antenna is somewhat more critical than when considering the NIC itself as an outer part of a matching circuit [8]. In this case, the antenna and the non-Foster circuit cannot be separated and the analysis made in [8], based on classical Linvill theory [9], is no longer valid. This theory suffer from two drawbacks, first of all, the analysis on “open-circuit stable” (OCS) or “short-circuit stable” (SCS) criterion constitute a necessary but non-sufficient condition for stability analysis, and secondly, as the non-Foster circuit is embedded in the antenna, there is no actual access to that point. In order to avoid that problem a different stability analysis is undertaken.

The stability analysis of the antenna loaded with a non-Foster network requires the use of methods that does not only include a reduced 2-port version of an  $N$ -node network but some of the possible poles of the whole antenna system [17]. Such an  $N$ -node network can be described by a matrix equation in the frequency domain:  $s = \sigma + j\omega$  [18]:

$$Y(s) \cdot V(s) = I(s) \quad (6)$$

Where  $Y(s)$  is an  $N \times N$  square matrix and  $I(s)$  and  $V(s)$ , are respectively excitation and response column vectors of size  $N$ . The whole circuit (antenna+NIC) will be stable if and only if all the poles of the system (roots of  $|Y(s)|$ ) lie in the *Left-Half-Plane* (LHP); otherwise the transient response will exhibit an exponential growth leading to instability [19]. A complex function called normalized determinant function NDF is defined as (7).

$$NDF(s) = |Y(s)| / |Y_0(s)| \quad (7)$$

Where  $|Y(s)|$  is the determinant of the studied circuit, and  $|Y_0(s)|$  is the determinant of the same circuit but with all the dependent generators (active elements) switched off. It is possible to determine the number of zeroes of the NDF in the RHP as the number of encirclements of the NDF around the origin in the complex plot. The system will be stable if the NDF does not encircle the origin when it is evaluated from  $\omega = -\infty$  to  $\omega = \infty$  [18]. One advantage of the NDF is that it can be easily

computed using any circuit software, by replacing each active device with its linear transconductance model and evaluating the response of its dependent node to an external excitation of magnitude 1.

### D. Step 4: Radiation considerations

According to the antenna structure and the selected NIC topology, the current distributions can change, and different modes can be excited once a non-Foster network is placed. This phenomenon is more arresting for planar structures [16]. In a linear structure, (e.g. dipoles and loops) the currents along the antenna do not change when an ideal purely reactive realization of  $Z_{NIC}^{an}$  is placed along the antenna. Nevertheless the resistive part of a real non-Foster network realization, unavoidable in practice, will produce some changes in the radiation pattern that must be considered in the design process.

### E. Step 5: Components' Tolerance effects

Additionally, and complementary to sensitivity and stability analysis, a study about the influence of the tolerance of resistors and capacitors in the impedance response of the NIC and the stability of the antenna system would be profitable. The easiest way to do that is through a CAD software with the option of yielding analysis where a confidence interval around the nominal values of each component (e.g. normal distribution for the nominal values in lumped elements with some tolerance percentage given by the manufacturer) can be set up. Moreover, it is possible to include parameters of the transistors' linear model, physical lengths of the layout and package parasitic. Iterative simulations take place automatically, and the results can be evaluated by graphic inspection or by numeric calculation of the deviation from some interval of interest, e.g. the  $S_{11}$  parameter over the intended bandwidth.

The importance of tolerance analysis does not rely on the statistic calculation around nominal values; it does in the identification of those parameters that have the most influence on the expected performance of the whole antenna system, providing reliability and higher control for the designer.

## III. DESIGN EXAMPLE

A printed small semi-loop, with a radius  $R = 40$  mm in a FR4 substrate with a thickness of 0.5 mm,  $\epsilon_r = 4.4$  and loss tangent  $\tan\delta = 0.02$ , is selected since the objective is to obtain an impedance matched dual-band small antenna, with a monopole-like radiation pattern at the lower band (i.e. VHF-band up to 200 MHz) as well as a simple and low-cost construction. The proposed antenna is an ESA for frequencies up to 840 MHz since the factor  $ka < 0.5$ , where  $a$  is the radius of the smallest sphere enclosing the antenna system ( $1.5 \cdot R$  in the current design) at the resonance frequency  $\omega_0$ , and  $k$  is the free-space wavenumber (i.e.  $k = \omega_0/c$ ) [13]. The antenna and the embedded non-Foster circuit are manufactured according to the proposed approach (see Fig. 3(a)). The first instance of the design process consists of checking the suitability of this structure to be

actively matched through *Sens* parameter, then a sweep of port 2 location is made using the CST® software, extracting a 2-port *S*-parameter matrix each time. A region with low sensitivity ( $|Sens| < 10$  dB) is found on the opposite side of the input port, near to the ground plane, as depicted in Fig. 3(b). *Sens* parameter was computed as the average of (5) over a frequency range from 10 to 300 MHz.

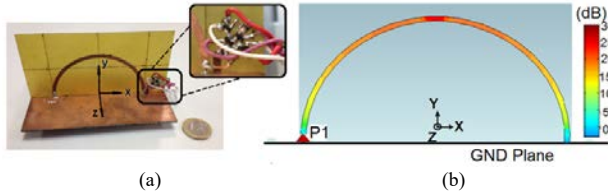


Fig. 3. Proposed small semi-loop. a.) Prototyped antenna with the embedded NIC and b.) the averaged sensitivity *Sens* over the antenna structure.

Since the best location is near the ground plane, a grounded NIC topology will be easy to implement. In this sense, a grounded NII topology, first proposed by Kolev [10] has been selected. The circuit consists of two BF998 MOSFETs connected in the way shown in Fig. 4(a). There is a strong dependence of  $Z_{NIC}$  on the squared transfer-conductance  $g_m^2$ ; as shown in the equation inset in Fig. 4(a). These transistors have a constant forward transfer admittance up to 1 GHz and a transient frequency  $f_T = 1.9$  GHz but, as aforementioned in Section II-B, a non-Foster behavior at the input impedance of the NII ( $Z_{NIC}$ ) should be expected to appear at frequencies lower than 200 MHz, as can be confirmed with the change of slope in its imaginary part in Fig. 4(c). That reactance-slope change indicates the frequencies after which the gate-source parasitic capacitance  $C_{gs}$  dominates the impedance response at NIC's input port, so it will correspond approximately with the maximum impedance matching range, at the lower intended band. Moreover, at higher frequencies, the changing slope of  $Z_{NIC}^{an}$  makes this impedance difficult to fit with a NIC (NII in this case), as can be seen in Fig. 4(c). This condition explains the dual-band response of the antenna, as will be shown below, and limits the performance of an ultra-wide-band actively matched semiloop. In order to achieve a trade-off between simplicity and performance, a series *LC*-tank ( $L_L = 15$  nH,  $C_L = 55$  pF) is connected to the NII as load ( $Z_L$ ) to be negated and inverted, in order to compensate the inductive behavior of the semiloop at lower frequencies.

Those values of  $Z_L$  for the NII are found through comparison with the impedance response of  $Z_{NIC}^{an}$  at the selected port 2 location, as it is shown in Fig. 4(b). Although the real and imaginary parts are not identical respectively, it is possible to obtain significant impedance bandwidths; this is the benefit of loading the antenna with the NII in a low sensitivity location. In order not to degrade the radiation efficiency, a NIC circuit with a low real part (ideally zero) in its input impedance must be connected. The bias circuit consists of another two BF998 connected as current sources to provide the drain current to the NII's FETs.

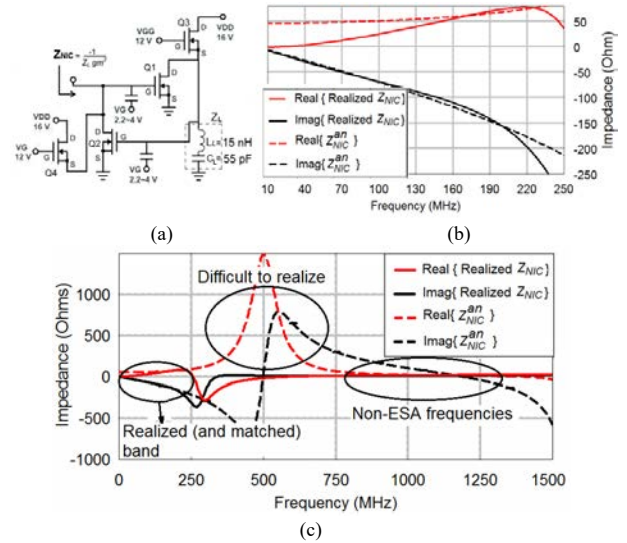


Fig. 4. a) Kolev's grounded NIC topology with FETs, where Q3 and Q4 are acting as current sources and b.) Its impedance response vs. the analytic one, computed as in (3), when port 2 is located at the opposite point from port 1. In this range of frequencies the semi-loop is an electrically small antenna. c.) A wider span comparing both impedances.

The stability test was performed using the AWR Microwave Office® suite to calculate the NDF and, at the same time, statistical analysis with a tolerance of 10% around the nominal values for all the components and transistor linear model parameters. The *S*-parameter model of the antenna was included in the calculus of the NDF. Figure 5(a) shows that the NDF calculated for the whole system does not encircle the origin of the root-locus plane, nor for the nominal values neither for the worst tolerance case (blurred lines), indicating stability condition for the design. However, low tolerance in NIC's components is preferable in a non-Foster approach. It was found that due to the strong relation between the impedance response and the bias point of the MOSFETs (through the parameter  $g_m^2$ ), small changes in DC biasing, especially in the gate-source voltage, produces more significant changes in antenna performance and stability than tolerance in lumped components.

The results, in terms of impedance matching, are shown in Fig. 5(b). Over a bandwidth of 140 MHz centered at 120 MHz an acceptable matching level is obtained (i.e.  $|S_{11}| < -8$  dB). The natural band of the unloaded antenna is not greatly degraded. In terms of miniaturization, values in the range 0.04 to 0.17 for the  $ka$  factor were reached at frequencies from 47 MHz to 187 MHz.

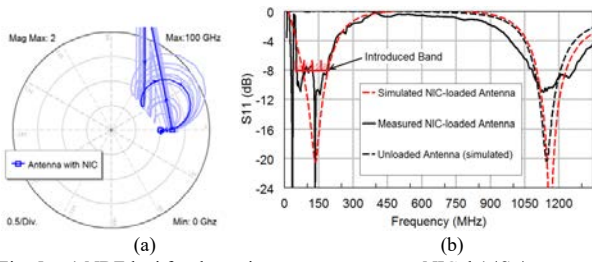


Fig. 5. a.) NDF loci for the entire system: antenna + NIC. b.)  $|S_{11}|$  response for the manufactured active matched semi-loop.

It is worth noting that, at frequencies near the semiloop resonance (i.e. at 1200 MHz, since  $R = 40$  mm), the current distributions over the antenna, depicted in Fig. 6(a) and (b), do not have significant changes, and a counter-phase current, flowing from the ground plane through the NIC and from the input port, generates a double-lobe pattern, as expected for the wavelength loop antenna (i.e. over the polar axis of the loop,  $z$ -axis), as can be seen in the measured results in Fig. 6(c). This condition corresponds to the fact that, at higher frequencies, the magnitude of the realized NIC impedance  $|Z_{NIC}|$ , decreases greatly, as the current flowing through the NIC does. However, at 1200 MHz, the measured received power, for the NIC-loaded case, is 1.4 dB lower than the unloaded antenna, indicating a moderate effect in the antenna gain.

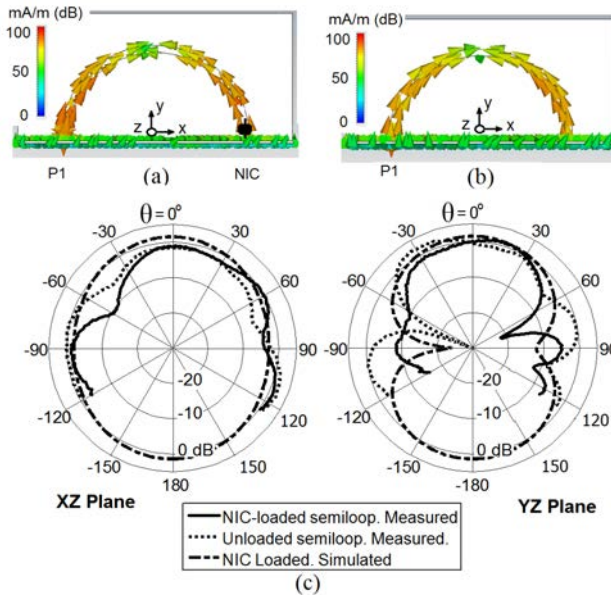


Fig. 6. Sketch of the current distributions at 1200 MHz for (a) the loaded and (b) the unloaded semiloop. (c) Measured radiation plot for both cases. In both planes the point  $\theta = 0^\circ$  agrees with the polar axis of the semiloop ( $z$ -axis).

For frequencies in the new lower band, where the NIC is acting as an active MN, a radiation pattern without significant changes should be expected. However, the unavoidable condition of nonzero real part in the realization of  $Z_{NIC}^{an}$ , produces a slight increase in the current over the semi-loop at the input port side (Fig. 7(a)). This leads to a lobe centered at the negative part of the  $x$ -axis ( $\Phi = 180^\circ$ ), in comparison with the unloaded case in Fig 7(b), as can be seen in the simulated

radiation pattern in Fig. 7(c). This condition can be considered as a design constraint and it cannot be omitted in the design process.

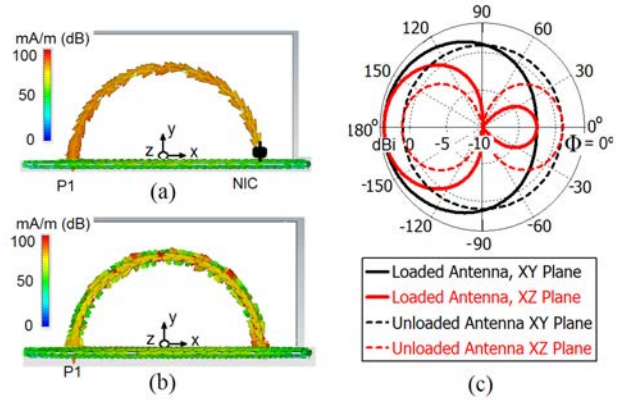


Fig. 7. Sketch of the current distributions at 125 MHz for (a) the loaded semiloop and (b) the unloaded semiloop. (c) Simulated directivity plot for both cases.

With the aim to complement the radiation considerations, the simulated directivity patterns, for frequencies within the introduced lower band, that is 100 MHz and the edge frequencies (50 MHz and 200 MHz) are depicted in Fig. 8. For those frequencies, the active-matched loaded semiloop shows similar radiation patterns. However, higher values of the resistive part of the realized NIC impedance may imply a more influenced radiation pattern at frequencies where the NIC is working as an active MN.

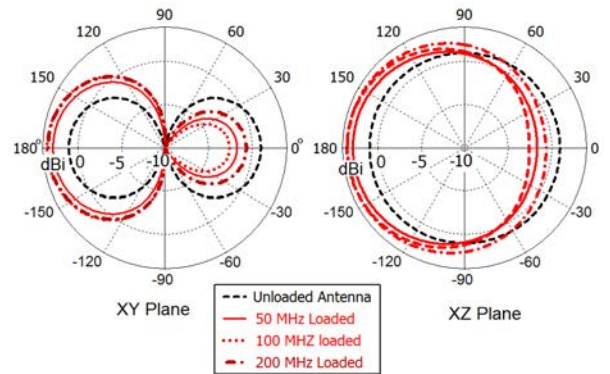


Fig. 8. Simulated directivity plot for the active matched semi-loop at different frequencies in the introduced lower band.

Finally, a power-budget in the VHF-band at 125 MHz has been undertaken. A known reference antenna is used as a transmitter  $T_x$  while the antenna under test is located for receiving at  $\theta = -90^\circ$ ,  $\Phi = 180^\circ$ , that is, in a direction parallel to the semiloop ground plane. This test-site resulted in an effective gain (see [20] and [21]) of the NIC-loaded antenna,  $G_{NIC-loaded}$ , of  $-6.88$  dB. From this figure it can be inferred that the radiation efficiency ( $\eta_{rad}$ ) for the loaded case is 10.91%, calculated from the relation  $G = \eta_{rad} D_{max}$ , where  $D_{max}$  is 2.7 dBi and corresponds with the simulated value for the loaded semiloop structure in the direction of interest, taking into account the changes in the directivity for this case, as aforementioned and depicted in Fig. 7(c). In the unloaded case, where the simulated

$D_{max}$  is 1.45 dBi, the measured gain  $G_{um}$  is -28.1 dB, and the calculated  $\eta_{rad}$  is 0.1%. If we now include the mismatching losses, we can calculate the total efficiency as  $\eta_{total} = \eta_{rad} \cdot (1 - |\Gamma_{in}|^2)$ . For the NIC-loaded case it results in  $\eta_{total\_NIC} = 0.109 \cdot (1 - |0.35|^2) = 9.6\%$ , while for the unloaded case it results in  $\eta_{total\_un} = 0.001 \cdot (1 - |0.98|^2) = 0.004\%$ . This result shows the improvement in radiation performance of the NIC-loaded antenna, for a single frequency and in a single Rx direction.

#### IV. CONCLUSION

A design methodology, with additional criteria to the conventional process, for actively matched antennas loaded with non-Foster networks, has been proposed. New sensitivity parameter *Sens* has been introduced in order to check, in a smart an automated way if the desired antenna is suitable or not for being matched with a non-Foster circuit. It is worth pointing out that any antenna structure can be studied under this strategy previously to be prototyped, saving time and effort. Additionally, considerations about tolerance in components have been shown to be profitable in order to identify sensitive parameters, not only in lumped components values but in manufacturing and set-up stages in the antenna plus MN system, which are studied as a unique entity. The NDF has been used to complement the methodology with a remarkable and easy to calculate alternative to predict the stability of the whole antenna system. Finally, considerations of radiation performance, one of the most challenging topics in embedded active matching design, have taken place since there are unavoidable responses in real non-Foster networks that produce changes, worthy of consideration, with respect to the case of a single port unloaded antenna. Those changes have to be taken into account in order to reach the application specifications.

#### REFERENCES

- [1] H. A. Wheeler, "Fundamental limitations of small antennas," *Proc. IRE*, vol. 35, no. 12, pp. 1479–1484, Dec. 1947.
- [2] L. J. Chu, "Physical limitations of omni-directional antennas," *J. Appl. Phys.*, vol. 19, no. 12, pp. 1163–1175, Dec. 1948.
- [3] H. L. Thal, "New radiation Q limits for spherical wire antennas," *IEEE Trans. Antennas Propag.*, vol. 54, no. 10, pp. 2757–2763, Oct. 2006.
- [4] H. W. Bode, *Network Analysis and Feedback Amplifier Design*. New York, USA: Van Nostrand, 1945.
- [5] R. M. Fano, "Theoretical limitations on the broadband matching of arbitrary impedances," *J. Frankl. Inst.*, vol. 249, no. 1, pp. 57–83, 1950.
- [6] D. C. Youla, "A New Theory of Broad-band Matching," *IEEE Trans. Circuit Theory*, vol. 11, no. 1, pp. 30–50, Mar. 1964.
- [7] R. M. Foster, "A reactance theorem," *Bell Syst. Tech. J.*, vol. 3, no. 2, pp. 259–267, Apr. 1924.
- [8] S. E. Sussman-Fort and R. M. Rudish, "Non-Foster Impedance Matching of Electrically-Small Antennas," *IEEE Trans. Antennas Propag.*, vol. 57, no. 8, pp. 2230–2241, Aug. 2009.
- [9] J. G. Linvill, "Transistor Negative-Impedance Converters," *Proc. IRE*, vol. 41, no. 6, pp. 725–729, Jun. 1953.
- [10] S. Kolev, B. Delacressonniere, and J.-L. Gautier, "Novel Microwave Negative Capacitance. Application to a Wide-Range Tunable Capacitance," in *Microwave Conference, 2000. 30th European*, 2000, pp. 1–3.
- [11] A. D. Harris and G. A. Myers, "An investigation of broadband miniature antennas," DTIC Document, 1968.
- [12] H. Mirzaei and G. V. Eleftheriades, "A Resonant Printed Monopole Antenna With an Embedded Non-Foster Matching Network," *IEEE Trans. Antennas Propag.*, vol. 61, no. 11, pp. 5363–5371, Nov. 2013.
- [13] N. Zhu and R. W. Ziolkowski, "Broad-Bandwidth, Electrically Small Antenna Augmented With an Internal Non-Foster Element," *IEEE Antennas Wirel. Propag. Lett.*, vol. 11, pp. 1116–1120, 2012.
- [14] M. Barbuto, A. Monti, F. Bilotti, and A. Toscano, "Design of a Non-Foster Actively Loaded SRR and Application in Metamaterial-Inspired Components," *IEEE Trans. Antennas Propag.*, vol. 61, no. 3, pp. 1219–1227, Mar. 2013.
- [15] S. Koulouridis, "Non-foster circuitry design for antennas," in *Antennas and Propagation (EUCAP), Proceedings of the 5th European Conference on*, 2011, pp. 237–239.
- [16] F. Albarracin-Vargas, E. Ugarte-Muñoz, V. González-Posadas, and D. Segovia-Vargas, "Sensitivity Analysis for Active Matched Antennas With Non-Foster Elements," *IEEE Trans. Antennas Propag.*, vol. 62, no. 12, pp. 6040–6048, Dec. 2014.
- [17] E. Ugarte-Munoz, D. Segovia-Vargas, V. Gonzalez-Posadas, and J. L. Jimenez-Martin, "Non-Foster matching of Electrically Small Antennas. Stability considerations," in *2012 IEEE Antennas and Propagation Society International Symposium (APSURSI)*, 2012, pp. 1–2.
- [18] A. Platzker and W. Struble, "Rigorous determination of the stability of linear N-node circuits from network determinants and the appropriate role of the stability factor K of their reduced two-ports," in *Integrated Nonlinear Microwave and Millimeterwave Circuits, 1994., Third International Workshop on*, 1994, pp. 93–107.
- [19] E. Ugarte-Munoz, S. Hrabar, D. Segovia-Vargas, and A. Kiricenko, "Stability of Non-Foster Reactive Elements for Use in Active Metamaterials and Antennas," *IEEE Trans. Antennas Propag.*, vol. 60, no. 7, pp. 3490–3494, Jul. 2012.
- [20] D. Segovia-Vargas, D. Castro-Galán, L.E. García-Muñoz and V. González-Posadas; "Broadband Active Receiving Patcha with Resistive Equalization", *IEEE Trans. on Microwave Theory and Techniques*, vol. 56, no. 1, pp. 56–64, Jan. 2008.
- [21] A. J. Simmons and D. G. Bodnar, "Gain of active antenna systems: Antenna standards committee requests input," *IEEE AP-S Newslett.*, pp. 62–64, Oct. 1989.